NAVAL POSTGRADUATE SCHOOL
Monterey, California

LEVEL II

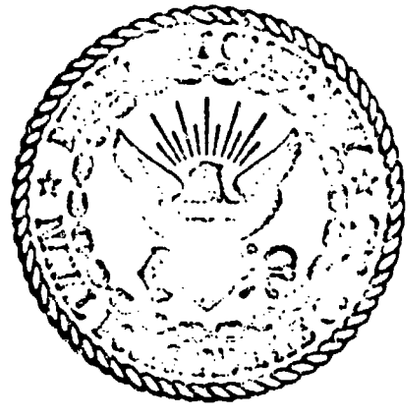

THESIS

TRANSVERSE OSCILLATIONS OF A CIRCULAR CYLINDER IN UNIFORM FLOW

by

David William Meyers

December 1975

Thesis Advisor: T. Sarpkaya

Approved for public release; distribution unlimited.

SECURITY CLASSIFICATION OF THIS PAGE (When Data Entered)

REPORT DOCUMENTATION PAGE

1. REPORT NUMBER	2. GOVT ACCESSION NO.	3. RECIPIENT'S CATALOG NUMBER

4. TITLE (and Subtitle)

(6) Transverse Oscillations of a Circular Cylinder in Uniform Flow,

AD49 825

5. TYPE OF REPORT & PERIOD COVERED

(9) Master's Thesis; December 1975

6. PERFORMING ORG. REPORT NUMBER

7. AUTHOR(s)

(10) David William Meyers

8. CONTRACT OR GRANT NUMBER(s)

9. PERFORMING ORGANIZATION NAME AND ADDRESS

Naval Postgraduate School
Monterey, California 93940

10. PROGRAM ELEMENT, PROJECT, TASK AREA & WORK UNIT NUMBERS

11. CONTROLLING OFFICE NAME AND ADDRESS

(11) Naval Postgraduate School
Monterey, California 93940

12. REPORT DATE

Dec[redacted]75

13. NUMBER OF PAGES

56

14. MONITORING AGENCY NAME & ADDRESS(if different from Controlling Office)

Naval Postgraduate School
Monterey, California 93940

15. SECURITY CLASS. (of this report)

Unclassified

15a. DECLASSIFICATION/DOWNGRADING SCHEDULE

16. DISTRIBUTION STATEMENT (of this Report)

Approved for public release; distribution unlimited.

(12) 57 p.

17. DISTRIBUTION STATEMENT (of the abstract entered in Block 20, if different from Report)

18. SUPPLEMENTARY NOTES

19. KEY WORDS (Continue on reverse side if necessary and identify by block number)

Cable strumming
Transverse oscillations
Fluid forces
Drag and inertia coefficients

20. ABSTRACT (Continue on reverse side if necessary and identify by block number)

The mean in-line force and the time dependent transverse force acting on a circular cylinder undergoing periodic transverse oscillations in an otherwise steady flow was measured for various amplitudes and frequencies of oscillation at several steady flow velocities. The experiments were carried out in a recirculating water tunnel operating as a closed channel at the test section. The mean in-line force has been expressed in terms of a mean

DD FORM 1 JAN 73 1473 (Page 1)

EDITION OF 1 NOV 65 IS OBSOLETE
S/N 0102-014-6601

SECURITY CLASSIFICATION OF THIS PAGE (When Data Entered)

251 450

Drag coefficient C_{di} and plotted as a function of A/D and D/$\bar{V}$T. The time dependent transverse force has been expressed in terms of the Fourier-averaged drag and inertia coefficients C_{dl} and C_{ml} and plotted as functions of the relative amplitude A/D and the period parameter $\bar{V}$T/D. The results have shown that the mean in-line force is significantly larger than that corresponding to steady flow about a non-oscillating cylinder and that energy may be transferred to the oscillating cylinder from the fluid at or near the vortex-shedding frequencies for the A/D values tested.

Transverse Oscillations of a Circular Cylinder in Uniform Flow

by

David William Meyers
Lieutenant Commander, United States Navy
B.S., United States Naval Academy, 1963

Submitted in partial fulfillment of the
requirements for the degree of

MASTER OF SCIENCE IN MECHANICAL ENGINEERING

from the

NAVAL POSTGRADUATE SCHOOL

December 1975

Author David William Meyers

Approved by: Thesis Advisor

Chairman, Department of Mechanical Engineering

Academic Dean

ABSTRACT

The mean in-line force and the time dependent transverse force acting on a circular cylinder undergoing periodic transverse oscillations in an otherwise steady flow was measured for various amplitudes and frequencies of oscillation at several steady flow velocities. The experiments were carried out in a recirculating water tunnel operating as a closed channel at the test section. The mean in-line force has been expressed in terms of a mean drag coefficient $\bar{C}_{di}$ and plotted as a function of A/D and $D/\bar{V}T$. The time dependent transverse force has been expressed in terms of the Fourier-averaged drag and inertia coefficients C_{dl} and C_{ml} and plotted as functions of the relative amplitude A/D and the period parameter $\bar{V}T/D$. The results have shown that the mean in-line force is significantly larger than that corresponding to steady flow about a non-oscillating cylinder and that energy may be transferred to the oscillating cylinder from the fluid at or near the vortex-shedding frequencies for the A/D values tested.

TABLE OF CONTENTS

LIST OF FIGURES

NOMENCLATURE

A	amplitude of cylinder oscillation
$\bar{C}_{di}$	mean in-line drag coefficient
C_{dl}	Fourier-averaged drag coefficient (Lift direction)
C_{ml}	Fourier-averaged inertia coefficient (Lift direction)
D	diameter of test cylinder
F	instantaneous total force acting on test cylinder
T	period of oscillation
t	time
U	instantaneous velocity
U_m	maximum velocity in a cycle ($U_m=2\pi A/T$)
$\bar{V}$	mean velocity of the uniform flow
A/D	dimensionless amplitude ratio
$D/\bar{V}T$	dimensionless frequency parameter
$\bar{V}T/D$	dimensionless period parameter
Re	Reynolds number ($Re=\bar{V}D/\nu$)
θ	phase angle
ν	fluid kinematic viscosity
ρ	fluid density

ACKNOWLEDGEMENT

I wish to express my sincere appreciation to Professor Turgut Sarpkaya for his encouragement and guidance throughout the period of research.

It is also a pleasure to acknowledge the help given by the personnel of the machine shop of the Department of Mechanical Engineering in constructing the testing apparatus. In particular, I wish to acknowledge the superb technical efforts of Mr. J. McKay in the construction of this system.

I. INTRODUCTION

Elastic structures of one or more degrees of freedom can extract energy from the flow about them and can develop catastrophic flow-induced vibrations. The understanding of this energy-extraction process is of paramount importance if one is either to eliminate or minimize it or to design the elastic structure such that it can withstand the oscillations under the contemplated environmental conditions.

Even a superficial familiarity with the parameters involved in this type of phenomenon shows that the investigation of the flow-induced vibrations or the flow about oscillating bodies is more than an extension of the past studies on flow about bluff bodies at rest. In fact, the complexity of the problem is increased by an order of magnitude. In view of this fact, it is no wonder that the past decade has produced either numerous experimental data with the goal of obtaining ad-hoc solutions for specific problems, while directing little if any attention toward elucidation of the underlying mechanics and toward generalization of the results for future applications; or numerous analytical models most or all of which had nothing to do with the motion of the very medium which provided the necessary energy to set the body in motion. In fact, the fluid mechanics of the flow-induced oscillations became so incidental to the phenomenon that the models dealt essentially with black-box-induced oscillations. To be sure, these models heavily relied on experimental data partly to justify

their existence and partly to assign numerical values to numerous variable constants imbedded in them. The ability of these models to scale, i.e., to permit extrapolation, is uncertain. Thus, in the final analysis one is not quite sure whether one should use the experimental data within the range of their application or the curves fitted to them by the empirical models. Suffice it to say that the phenomenon is far from understood even for the idealized conditions encountered in the laboratory without the alarming consequences of the real ocean environment where fauna and flora, ever-changing ocean currents, and temperature gradients add further complications to an already complex problem. Surely, over design is not the answer but it may, in the next decade or so, be the best available tradeoff with failure.

Mathematical models of flow-induced vibrations of bluff bodies and the response of circular cylinders to vortex shedding have been aptly described by Parkinson [1] and Currie, et al. [2] and will not be repeated here.

It appears that among the various models considered so far, the "wake-oscillator" model of Hartlen and Currie [3] attracted more attention among the students of vibration analysis. We will not elaborate here on the attempts made by others to introduce one or more additional terms into the model originally proposed by Hartlen and Currie for such naive attempts produced only more papers and unrealistically defined coefficients than sound information toward the understanding of the flow-induced oscillations both in-line with and transverse to the ambient flow.

It suffices to conclude that despite the extensive attention given to the study of the transverse oscillations of bluff bodies in air and water, there has been very little or no attempt to measure the forces acting on the bodies and to separate the time-dependent force into suitable components. It has, however, been firmly established that there is a band of frequencies in the vicinity of the Strouhal frequency in which the vortex shedding is synchronized or locked-in and that both the intensity of the vortex shedding and the spanwise correlation are enhanced. The synchronization or lock-in is manifested by a rapid decrease in inertial force and a rapid increase in the absolute value of the drag force. In other words, the total force which is nearly in-phase with the motion before synchronization becomes nearly out of phase at and after synchronization.

The purpose of the present investigation is the determination of these in-phase and out-of-phase components of the time dependent force acting on cylinders undergoing transverse oscillations in a uniform stream and the correlation of the normalized force components with appropriate governing parameters through the use of an equation proposed herein. Evidently, it is through the understanding of the forces acting on oscillating bodies that one would eventually be able to devise models to predict the strumming or the hydroelastic behavior of rigid or elastic bodies immersed in fluid streams.

II. EXPERIMENTAL APPARATUS AND PROCEDURE

A. EQUIPMENT

1. NPS Water Tunnel

The experiments were performed in a recirculating water tunnel (Figure 1) which had a capacity of approximately 500 gallons. The galvanized test section, four inches wide, eight inches high and sixteen inches long, was closed on top with a removable plexiglass plate to eliminate the free surface effects. A small space adjacent to the side walls was provided to allow the passage of thin leaf arms connecting the cylinder, in the test section, to the driving hardware above the test section. A low RPM, high capacity, fourteen-inch-diameter-discharge centrifugal pump was used to circulate the fluid through the test section. The velocity of the fluid was regulated by a butterfly valve arrangement situated downstream of the test section. Velocities of 0.8 to 1.4 feet-per-second were obtained by adjusting the vanes of the butterfly valve.

2. Motor, Flywheel and Pivot Assembly

The periodic motion in this experiment was obtained by the use of a small, variable speed, electric motor, a flywheel and pivot assembly (Figure 2). The electric motor, mounted so as to isolate its vibrations from the remainder of the test apparatus, transmitted rotary motion through a flexible belt to a flywheel. A 56 inch long, rigid bar, pivoted at its center, transmitted the vertical component of motion of a bearing, attached to the flywheel, to a shaft connected

Figure 1. NPS water tunnel.

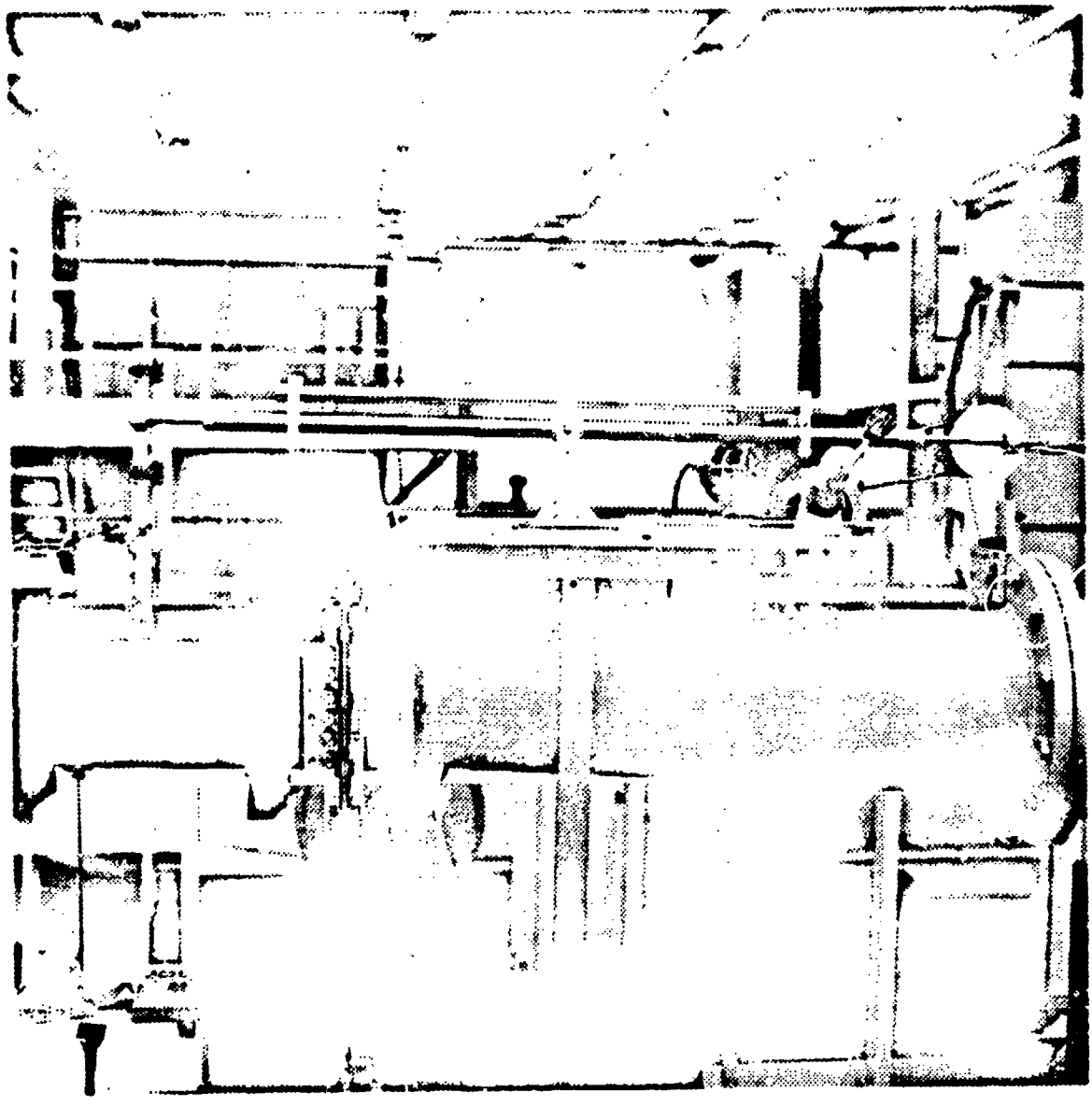

Fig. 2 Motor, Flywheel and Pivot Assembly

to the yoke assembly and cylinder. Horizontal motion was expended at both ends of the pivot rod by the free motion of bearings along the pivot arm. The amplitude, "A", of the vertical periodic motion was set by adjusting the radial position of the bearing attached to the flywheel. For these experiments, the amplitude ranged from 0.25 to 0.75 inches. The frequency of oscillation was regulated up to four cycles per second by adjustment of the variable speed motor. The system was designed and constructed to produce essentially sinusoidal oscillations, free of secondary oscillations.

3. Test Specimen and Yoke Assembly

A one-inch diameter circular cylinder, constructed of aluminum tubing, was used as the test specimen. The cylinder was held in the test section by a yoke assembly which was connected to the pivot arm by means of a vertically constrained rod. The action of the pivot arm caused the cylinder to oscillate vertically in the test section, transverse to the stream flow. The aluminum yoke assembly/force transducer (Figure 3) was instrumented with the strain gages and accelerometers required to monitor the forces and the acceleration felt by the cylinder.

4. Sensors and Sensor Support

The mean velocity of the fluid was derived from the pressure differential of a pitot tube installed in the test section upstream of the test cylinder. One channel of a two channel recorder was used to continuously monitor the stream velocity during experiments. The calibration of the pitot

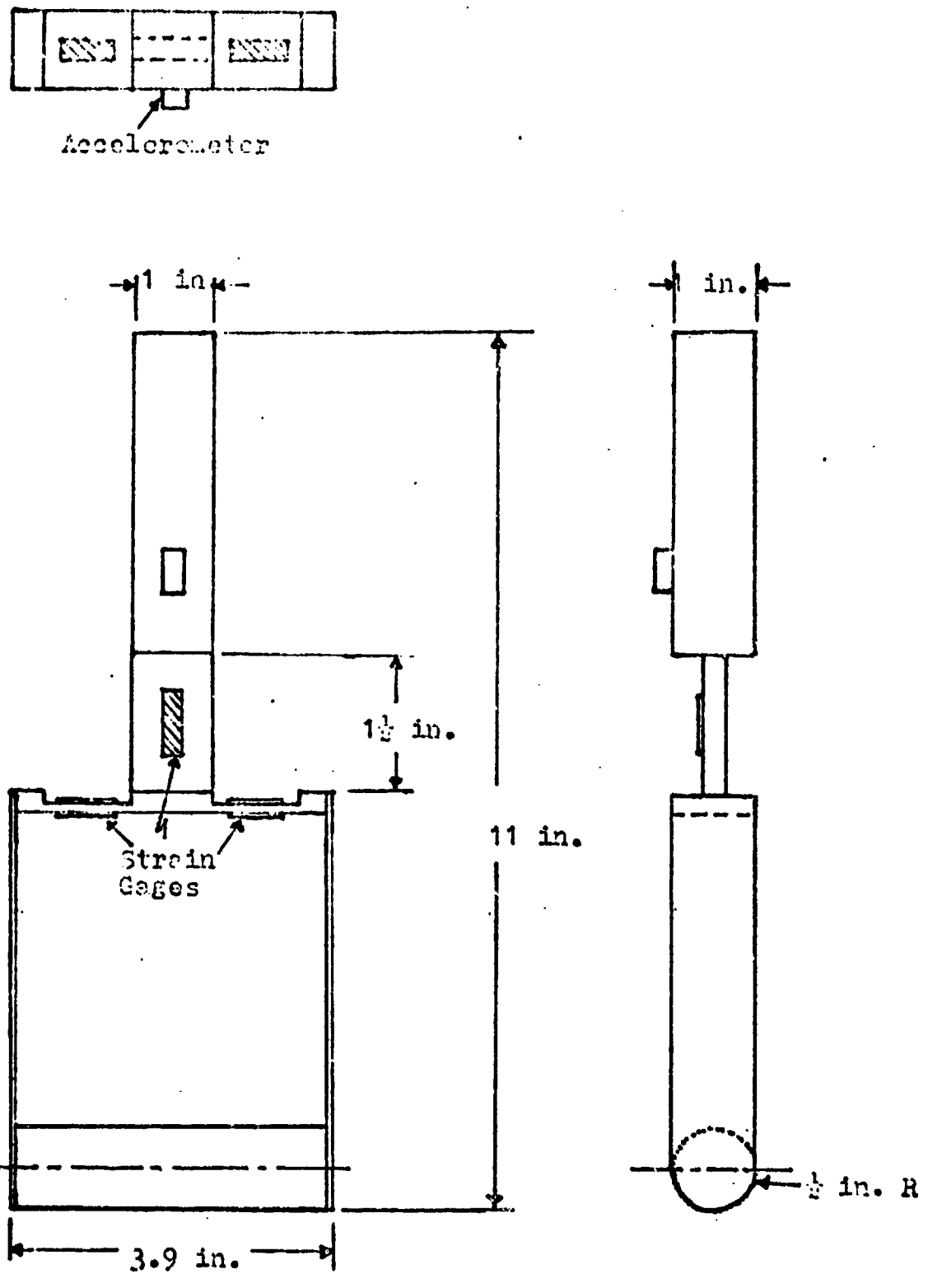

Fig. 3 Aluminum Yoke—Force Transducer

tube and transducer was accomplished by means of a water bottle and precisely measured plates which were used to produce a known water height differential.

The instantaneous acceleration of the pivot arm was sensed by an accelerometer mounted on a yoke assembly. The acceleration signal was processed through a filter, to remove high frequency vibrations, and was recorded on one channel of a two channel recorder.

Instantaneous forces were sensed by four piezo-resistive strain gages. A cantilever beam type arrangement, forming the top of the yoke assembly, as seen in figure 3, provided the mounting location for the strain gages. The forces sensed by this force transducer system were recorded on the two channel recorder. Calibration of the force transducer system was accomplished by hanging loads at the mid-section of the cylinder, supported at the correct orientation so as to calibrate for vertical forces for the transverse or lift force measurements, and then for the horizontal, or in-line force measurements.

B. PROCEDURE

System checkout and sensor calibration preceded the experimental runs. Several test runs were made to verify the proper operation of the test system, sensors, processing and recording equipment, and to establish the test run procedures to be used. It was verified that the mechanical system produced the required periodicity of oscillation for frequencies

below about three cycles per second and amplitudes below one inch. It was decided that the system would not be driven at higher frequencies or larger amplitudes during the test runs because of the presence of excessive vibrational effects beyond these limits. It was verified that the sensors and processing equipment had adequate sensitivity and phase reproduction to allow measurement of the required physical parameters.

The first set of experiments has as an objective, the measurement of the mean fluid-induced force on the cylinder, in the direction of the stream flow, (in-line force) for various frequencies and amplitudes of cylinder oscillation transverse to the stream flow. It was verified by experiment that there was no in-line component of inertial force.

The physical recording of the in-line force was accomplished with the Honeywell recorder. Pitot differential pressure was recorded simultaneously to verify the magnitude and constancy of fluid velocity during the runs. Accelerometer output was recorded on the two channel recorder to provide data on oscillation period and phase angle. The flow velocity was set at 0.84 feet per second, the amplitude at 0.25 inches, and the data runs were taken as the oscillation frequency was varied from zero to about three cycles per second. The charts were annotated with run data for later correlation. The procedure was repeated for amplitudes of 0.5 and 0.75 inches and the entire series was repeated again at a flow velocity of 1.3 feet per second.

Subsequently, the mean in-line force, the flow velocity, the oscillation period and amplitude, and the cylinder diameter were recorded from the charts. A mean drag coefficient $\bar{C}_{di}$ was manually calculated from this data for correlation with the frequency parameter $D/\bar{V}T$ and the nondimensionalized amplitude A/D.

The second set of experiments had as an objective the measurement of the time dependent forces in the direction of cylinder motion, i.e., transverse to the direction of stream flow. Since, in this case, there was an inertial force in the direction of interest, it was necessary to adjust the experimental procedure in order to identify the instantaneous value of the inertial force. Separation of the inertial force from the total force measured with the cylinder submerged, was required to ascertain the resistive force produced by the fluid alone.

The physical recording of the transverse force was accomplished using one channel of the two channel recorder. Acceleration was measured simultaneously on the other channel. The water level in the tunnel was alternately raised and lowered for each run in order to allow recording of the total "Wet" force and the inertial "Dry" force at a common frequency and amplitude of oscillation. The acceleration trace provided the reference for the time correlation of the wet and dry force data. Because of the necessity to properly correlate wet and dry phase information, extreme care was taken in verifying the zeros for the acceleration and force recordings.

Since the time dependent force was of interest, the mean force and acceleration was used as the respective trace zeros. This value was found by electrically averaging the force and acceleration signals, and setting the resultant mean value to a convenient position on the recording trace. The flow velocity was initially set at 0.84 feet per second, the amplitude at 0.25 inches, and runs were taken for various oscillation frequencies up to about three cycles per second. The procedure was repeated for amplitudes of 0.5 and 0.75 inches and then the entire series was repeated at a new flow velocity of 1.33 feet per second. Figure 4 shows the force and acceleration traces for a typical experimental run.

From traces similar to figure 4, the transverse force was read and recorded from both the wet and dry run curves. Starting from the zero acceleration time (illustrated on figure 4) the wet and dry forces were recorded each 0.01 second, for at least three complete cycles. This data was then punched on IBM computer cards for evaluation.

The computer program for calculating the transverse drag and inertia coefficients, given in Appendix A, was also used, along with visual inspection, to determine the goodness of the data and the accuracy of the data retrieval procedures. Computed values of the mean wet and dry forces, if significantly different from zero, indicated possible errors in the establishment of system zeros or the presence of secondary undesirable effects from the mechanical system. After completion of this data assessment, the drag and inertia coefficients were

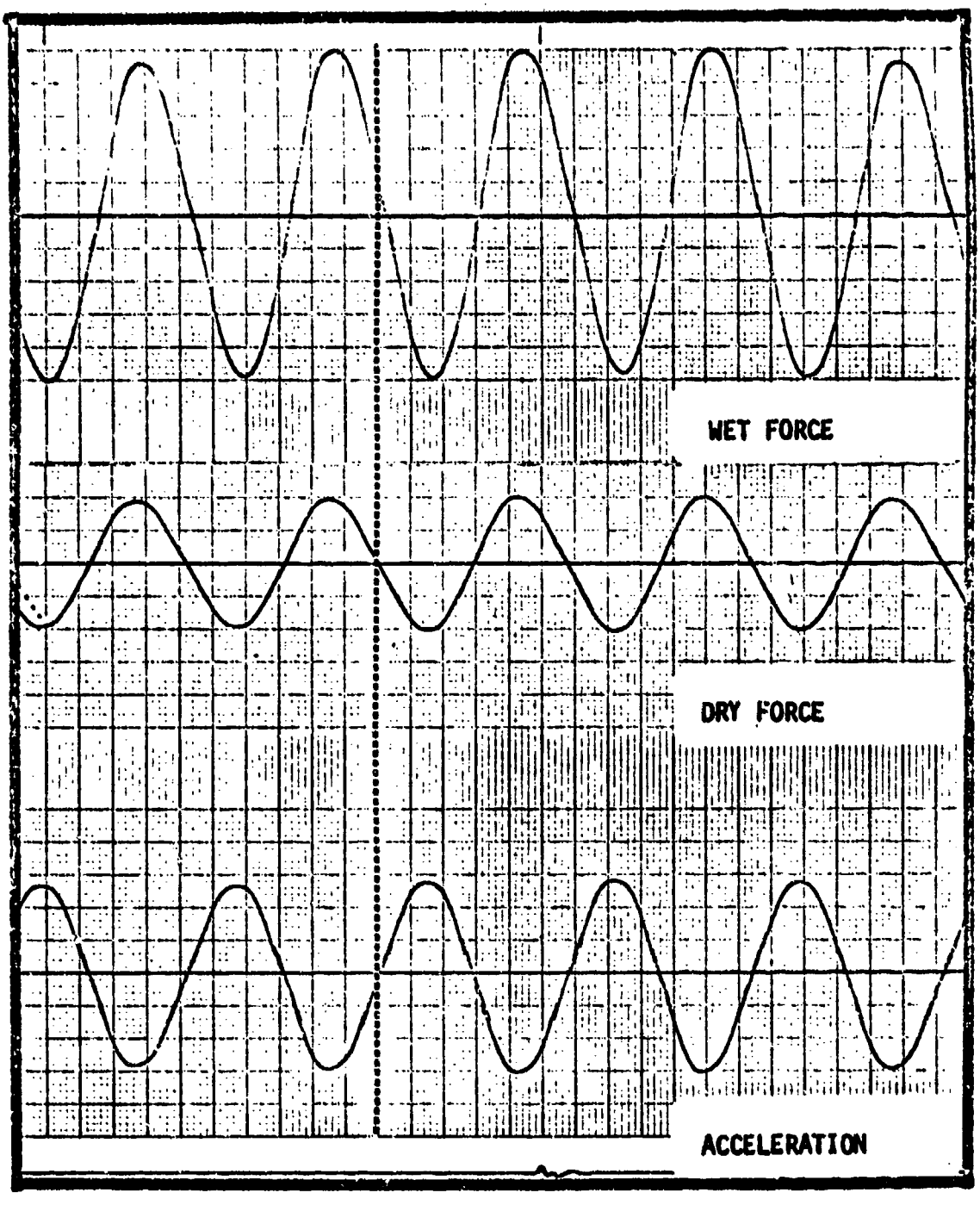

Fig. 4 Force and Acceleration Traces

calculated and recorded as a function of the period parameter $\bar{V}T/D$ for the three values of the nondimensionalized amplitude A/D investigated.

III. DATA ANALYSIS

The numerical calculations as well as measurements in time-dependent flow yield the resultant force as a function of time for a given set of numerical values of the independent parameters. Thus it is not possible without a suitable hypothesis, to express the force both as a function of time and remaining independent parameters as one ordinarily would in a closed form solution. Such a working hypothesis is particularly necessary for the cable strumming problem since the results are to be incorporated into the dynamics of the cylinder motion in the form of a forcing function. It should be stated at the outset that there is, at present, no generally accepted hypothesis to decompose the time dependent force into suitable components. As it will be seen shortly, even the existing hypotheses, such as the so-called Morison's equations, are not applicable to periodic flows with a non-zero mean velocity.

Stokes, in a remarkable paper on the motion of pendulums, showed that the expression for the force on a sphere oscillation in an unlimited viscous fluid consists of two terms, one involving the acceleration of the sphere and the other the velocity. This analysis shows that the inertia coefficient is modified because of viscosity and is augmented over the theoretical value valid for irrotational flow. The drag coefficient associated with the velocity is modified because of acceleration, and its value is greater than it would be if the

sphere were moving with constant velocity. In general, the force experienced by a bluff body at a given time depends on the entire history of its acceleration as well as the instantaneous velocity and acceleration. Thus, the drag coefficient in unsteady flow is not equal to that at the same instantaneous velocity in steady flow. Neither is the inertia coefficient equal to that found for unseparated potential flow. As yet a theoretical analysis of the problem for separated flow is difficult and much of the desired information must be obtained both experimentally and numerically. In this respect, the experimental studies of Morison and his co-workers [4] on the forces on piles due to the action of progressive waves have shed considerable light on the problem. The forces are divided into two parts, one due to the drag, as in the case of flow of constant velocity, and the other due to the acceleration or deceleration of the fluid. The concept necessitates the introduction of a drag coefficient C_d and an inertia coefficient C_m in the expression for force. In particular if F is the force per unit length experienced by a cylinder, then

$$F = 0.5\, C_d \rho D |U| U + C_m\, \rho \pi \frac{D^2}{4} \frac{dU}{dt} \qquad (1)$$

where U and dU/dt represent respectively the undisturbed velocity and the acceleration of the fluid.

On the basis of irrotational flow around the cylinder, C_m should be equal to 2 (cylinder at rest, the fluid accelerating; otherwise $C_m = 1$), and one may suppose that the value of C_d should be identical with that applicable to a constant

velocity. However, numerous experiments show that this is not the case and that C_d and C_m show considerable variations from those just cited above. Even though no one has suggested a better alternative, the use of the Morison's equation gave rise to a great deal of discussion on what values of the two coefficients should be used. Furthermore, the importance of the viscosity effect has remained in doubt since the experimental evidence published over the said period has been quite inconclusive.

The drag and inertia coefficients obtained from a large number of field tests, as compiled by Wiegel [5], show extensive scatter whether they are plotted as a function of the Reynolds number or the so-called period parameter U_mT/D. The reasons for the observed scatter of the coefficients C_m and C_d remained largely unknown. The scatter was attributed to several reasons or combinations thereof such as the irregularity of the ocean waves, free surface effects, inadequacy of the average resistance coefficients to represent the actual variation of the nonlinear force, omission of some other important parameter which has not been incorporated into the analysis, the effect of ocean currents on separation, vortex formation, and hence on the forces acting on the cylinders, etc.

The most systematic evaluation of the Fourier-averaged drag and inertia coefficients has been made by Keulegan and Carpenter [6] through measurements on submerged horizontal cylinders and plates in the node of a standing wave, applying

theoretically derived values for velocities and accelerations. Additional measurements have been made by Sarpkaya [7] of the in-line as well as transverse forces acting on cylinders and spheres in a sinusoidally oscillating fluid and it was found that the drag coefficient as well as the inertia coefficient for a strictly sinusoidally oscillating fluid (no mean velocity) is a function of $U_m T/D$ and that the effect of the Reynolds number is rather secondary and certainly obscured by the excellent correlation of the data with the period parameter $U_m T/D$.

On the basis of the above discussion, one would assume that Morison's equation would apply equally well to periodic flow with a mean velocity where $u = \bar{V} - U_m \cos\theta$ and that C_{dl} and C_{ml} will have constant, time-invariant, Fourier or least-squares averages. This, in turn, implies that C_{dl} and C_{ml} are independent of the associated flow phenomena. There is, however, no a priori assurance in the principles of fluid mechanics of theory of models that this is, in fact, the case. Thus the effect of the combination of a uniform current and harmonic oscillations on the time-average and oscillatory forces acting on circular cylinders will have to be re-examined and the limits of application of the Morison's equation be delineated.

It is a priori evident that both $u = -U_m \cos\theta$ and $u = \bar{V} - U_m \cos\theta$ yield the same acceleration du/dt. Thus, the force in-phase with the acceleration in Morison's equation

remains unaffected by the presence of the mean flow. The results presented herein show that this is not the case. Furthermore, the use of the Morison's equation as

$$F = 0.5\rho C_d(\bar{V}-U_m\cos\theta)\left|\bar{V}-U_m\cos\theta\right| + C_m\rho\pi\frac{D^2}{4}\frac{du}{dt} \qquad (2)$$

requires that the time-averaged drag force be calculated by increasing the force calculated from the steady flow by a factor $[1 + 0.5(U_m/\bar{V})^2]$. The results presented herein show that such an analysis appreciably underestimates the measured mean forces. It suffices to state that the fluid flow phenomena for bluff bodies are significantly affected by the combination of currents and harmonic oscillations and that the results for steady currents alone and oscillations alone cannot be combined to yield reliable estimates of forces due to both acting together.

The time-dependent forces per unit length in the present study are analyzed according to the following three-coefficient equation:

$$F = 0.5\bar{C}_d\rho D\bar{V}^2 + C_m\rho\pi\frac{D^2}{4}\frac{d}{dt}\left(-U_m\cos\frac{2\pi}{T}t\right) - 0.5\,C_d D U_m^2\rho\left|\cos\frac{2\pi}{T}t\right|\cos\frac{2\pi}{T}t \qquad (3)$$

which may be written as,

$$\frac{F}{0.5\rho D\bar{V}^2} = \bar{C}_d + C_m\pi^2(U_mT/D)(D/\bar{V}T)^2\sin\frac{2\pi}{T}t - C_d(U_mT/D)^2(D/\bar{V}T)^2\left|\cos\frac{2\pi}{T}t\right|\cos\frac{2\pi}{T}t \qquad (4)$$

in which C_m and C_d are given by their Fourier averages as

$$C_m = (2U_mT/\pi^3D)\int_0^{2\pi}(F\sin\theta)\,d\theta/(U_m^2D) \tag{5}$$

and

$$C_d = -(3/4)\int_0^{2\pi}(F\cos\theta)\,d\theta/(U_m^2D) \quad . \tag{6}$$

Evidently, C_d, C_m, and $\bar{C}_d$ are functions of $\bar{V}T/D$ and U_mT/D or A/D. They may depend also on the Reynolds number which does not explicitly appear in the above expression because of the assumptions made in the formulation of the basic force equation.

In the foregoing, neither the coefficient $\bar{C}_d$ is assumed to be equal to the steady-state drag coefficient for a uniform flow at the constant velocity $\bar{V}$, nor C_m and C_d are assumed to be identical to those obtained for a strictly harmonic oscillation. In fact, the results show that $\bar{C}_d = C_d$ (steady) only for $U_m = 0$, and C_d and C_m are equal to those obtained for the harmonic oscillation only for $\bar{V}T/D=0$.

The equation proposed above is general enough to be applicable to both in-line and transverse oscillations. In the case of transverse oscillations, however, the mean net force in the direction of oscillation is zero, i.e., $\bar{C}_d=0$, and thus, one has

$$\frac{F(\text{transverse force})}{0.5\rho\bar{D}V^2L} = C_{ml}\pi^2(U_mT/D/\bar{V}T)^2\sin\frac{2\pi}{T}t - C_{dl}(U_mT/D)^2(D/\bar{V}T)^2\left|\cos\frac{2\pi}{T}t\right|\cos\frac{2\pi}{T}t \tag{7}$$

In the foregoing, the inertia and drag coefficients have been denoted as C_{ml} and C_{dl} in order to distinguish them from those corresponding to in-line oscillations. The subscript "l" carries the meaning of "Lift" or force in the direction transverse to the stream.

Ordinarily, for a perfectly sinusoidal oscillation of the cylinder, the coefficients C_{ml} and C_{dl} would be given by equations (5) and (6). However, when the oscillations are not perfectly harmonic, it is relatively more accurate to use the velocities and the accelerations encountered in the experments rather than assuming them to be simple harmonic motions. It is with this objective in mind that the equations (5) and (6) were rewritten as

$$C_{ml} = \frac{2T}{\pi^2 D^2 \rho U_m} \frac{\int_0^{2\pi} F \sin\theta \, d\theta}{\int_0^{2\pi} \sin^2\theta \, d\theta} \tag{8}$$

and

$$C_{dl} = \frac{-T^2}{2\rho D \pi^2 A^2} \frac{\int_0^{2\pi} F \cos\theta \, d\theta}{\int_0^{2\pi} \cos^2\theta \, |\cos\theta| \, d\theta} \tag{9}$$

as they would be obtained from equation (3) in the usual application of the Fourier analysis. Evidently, had the oscillations been perfectly harmonic the integrals appearing in the denominators of the above equations would have reduced to

$$\int_0^{2\pi} \sin^2\theta \, d\theta = \pi \tag{10}$$

and

$$\int_0^{2\pi} \cos^2\theta \left|\cos\theta\right| d\theta = \frac{8}{3} \tag{11}$$

The equations (8) and (9) together with equations (10) and (11) would have reduced to equations (5) and (6).

Since in the present study the periodic oscillations were not perfectly sinusoidal partly by design in order to obtain greater generality and flexibility in the experimentation and partly due to the constraints imposed in the design of the oscillation mechanism, it became necessary to incorporate into equations (8) and (9) the exact form of the oscillations encountered in the experiments. For this purpose the dry force, which is an exact representation of the oscillations, was normalized as

$$f(\theta) = \frac{F\text{-dry}}{\left|F\text{-dry(maximum)}\right|} \tag{12}$$

and then the equations (8) and (9) were rewritten as

$$C_{ml} = \frac{2T}{\rho\pi^2 D^2 U_m} \frac{\int_0^{2\pi} F \cdot f(\theta)\, d\theta}{\int_0^{2\pi} f(\theta)\, d\theta} \tag{13}$$

and

$$C_{dl} = -\frac{T^2}{2\rho D\pi^2 A^2} \frac{\int_0^{2\pi} F \cdot f(\theta+\pi/2)\, d\theta}{\int_0^{2\pi} f(\theta+\pi/2)\left|f(\theta+\pi/2)\right| d\theta} \tag{14}$$

It is easy to show that equations (13) and (14) reduce to equations (8) and (9) or to equations (5) or (6) for purely harmonic oscillations for which $f(\theta) = \sin\theta$. The advantage of the use of the equations (13) and (14) is rather obvious for all types of periodic oscillations. Furthermore, the independent evaluation of the denominators of equations (13) and (14) and their comparison with π and 8/3 respectively (as they would have been equal to had the oscillations been harmonic) gave an indication of the deviation of the observed periodic oscillations from a purely harmonic oscillation.

The force acting on the cylinder in the in-line direction due to the oscillations in the transverse direction is expressed in terms of a mean drag coefficient, denoted by $\bar{C}_{di}$, given as

$$\bar{C}_{di} = \frac{\text{Force in the in-line direction}}{0.5\ \rho L D \bar{V}^2} \qquad (15)$$

Evidently, $\bar{C}_{di}$, C_{ml} and C_{dl} depend on $D/\bar{V}T$, $U_m T/D$ or $2\pi A/D$, and possibly on the Reynolds number.

The experimental data are analyzed using the computer program given in Appendix A written according to the equations (13), (14), and (15) and are plotted in terms of A/D and either $D/\bar{V}T$ or $\bar{V}T/D$.

IV. DISCUSSION OF RESULTS

The results will be discussed in two parts. The first will be the average in-line force acting on the cylinder undergoing forced periodic oscillations in the transverse direction. The second will be the time dependent transverse force.

Evidently, the average in-line force is coupled with secondary oscillations due to vortex shedding. However, such oscillations are rather small in both steady and periodic flows and certainly not larger than about seven percent of the average force. It is for this reason that only the average of the in-line force acting on the oscillating cylinder is presented here.

Figures 5, 6, and 7 show the variation of the normalized in-line force ($\overline{C}_{di}$) as a function of $D/\overline{V}T$ for A/D =0.25, 0.50 and 0.75 respectively. Each figure represents the data obtained with two velocities, namely, $\overline{V}$=0.84 and $\overline{V}$=1.3. In normalized form these velocities correspond, for the one inch cylinder used, to the Reynolds numbers $Re=\overline{V}D/\nu$ = 7000, and Re = 10,833.

Evidently, the in-line force increases with A/D since the cylinder, undergoing transverse oscillations, presents a larger apparent-projected area to the mean flow. This, however, is only part of the explanation. In addition, the vortex growth and motion are affected by the oscillation of the cylinder which in turn affect the in-line and transverse

forces acting on the cylinder. This is evidenced by the fact that the in-line force for a given A/D increases at first, reaches a maximum, and then decreases as $D/\bar{V}T$ increases. A simple minded calculation based on the steady flow drag coefficient for a stationary cylinder and the apparent projected area for the in-line force $\bar{F}$, which may be written as

$$\bar{C}_{di} = \frac{\bar{F}}{\frac{1}{2}\rho\bar{V}^2DL} = C_{ds}(1 + 2A/D)$$

yields values which are almost equal to the maximum values given in figures 5, 6, and 7. It should be noted, however, that the phenomenon is far more complex, and that such a simple minded procedure should not generally be used, even though the results are surprisingly good.

For the purposes of comparison, the figures 5, 6, and 7 are combined in figure 8 by drawing mean lines through the data points. Figure 8 shows that the in-line force coefficient reaches its maximum at $D/\bar{V}T$ between 0.18 and 0.20. Ordinarily, the Strouhal number for a stationary cylinder would be 0.22 for the Reynolds numbers cited previously, and one would expect that the forces acting on the cylinder will undergo dramatic changes as the vortex shedding frequency given by the Strouhal number coincides with the frequency of the cylinder oscillations. The present results show that such a synchronization takes place at a frequency slightly lower than the Strouhal frequency.

Also shown in figure 8 is the normalized amplitude of the oscillations in the in-line force for A/D=0.5. As noted

earlier the oscillations are quite negligible relative to the mean force and certainly under 7 per-cent. It should be noted that the amplitude of the oscillations, like the average force show an almost sudden increase in the vicinity of $D/\bar{V}T$ nearly equal 0.19 and remain at that value for larger values of $D/\bar{V}T$. The occurrence of synchronization as well as the increase of the amplitude of oscillations are shown most dramatically in figure 9. This figure was obtained by setting the free stream velocity at 0.84 feet per second and the A/D ratio equal to 0.5. Then, beginning with the case of the non-oscillating cylinder, the frequency of the oscillations was gradually increased up to about four cycles per second and the resulting in-line force was continuously recorded. The figure shows that the in-line force increases rapidly but with very little oscillations superimposed on it. As soon as the state of synchronization is reached, the amplitude as well as the frequency of the force oscillations increases.

From an engineering point of view the significance of the magnitude of the in-line force is that a cylinder or cable excited by the flow to oscillate in the transverse direction may be subjected to in-line forces several times larger than assumed in its design. Furthermore, the deflections caused by the in-line force on sufficiently flexible cylinders tend to couple with transverse ocsillations and not only affect the magnitude of the transverse oscillations but also the path of the cylinder motion. Thus it is not uncommon to see heat exchanger pipes or chimneys exhibit oscillation patterns in the plane normal to their axis.

The time dependent transverse force is described, as noted earlier, in terms of a drag coefficient C_{dl} and an inertia coefficient C_{ml} given by

$$\text{Transverse Force} = C_{ml}\frac{\rho\pi D^2}{4}\frac{d}{dt}(-U_m\cos\theta) - C_{dl}\rho\frac{DU_m}{2}^2\cos\theta|\cos\theta|$$

Figures 10, 11, and 12 show C_{dl} and C_{ml} as a function of $\bar{V}T/D$ for A/D - 0.25, 0.50 and 0.75 respectively. These coefficients were obtained without the $\bar{C}_d$ term in the generalized Morison equation (see equation 3) since the mean of the transverse force is zero.

It is seen from these figures that important variations in C_{dl} and C_{ml} occur particularly in the vicinity of the Strouhal frequency (here $\bar{V}T/D \cong 4.5$ to 7) where the natural eddy-shedding at the Strouhal frequency is both enhanced and correlated by the oscillations.

The inertia coefficient or the normalized in-phase component of the transverse force undergoes a rapid drop as the frequency of the oscillation approaches the Strouhal frequency from both the upper and lower limits. In other words, synchronization or lock-in is manifested by a rapid decrease in inertial force and a rapid increase in the absolute value of the drag force.

This fact, which has not been recognized before, shows that the lock-in phenomenon is a phase transformer. The total force which is nearly in phase with the motion before synchronization becomes nearly out of phase at or after synchronization. It should be noted in passing that the success

of many empirical models dealing with this type of oscillation comes partly from the manipulation of the phase angle near synchronization. It is now apparent that the fluid force to be used in the equations expressing the motion of a cylinder or cable should be given by the data presented herein. Such data take care, not only of the variation of the phase angle, but also the amplitude of the transverse force as a function of the normalized frequency.

Figure 13 depicts an example of the occurrence of synchronization as the period of oscillation is gradually decreased. The upper trace shows the phenomenon as frequency is increased from the non-oscillating case to just beyond the synchronization frequency. The lower trace provides an exploded view of the phenomenon near the synchronization frequency. The transverse force sharply decreases as soon as the point of synchronization is reached. Beyond that point, the changes in the transverse force with frequency are quite small. The phenomenon is reversible and one would obtain a figure similar to figure 13 if one gradually decreased the frequency. The possibility of the occurrence of an hysteresis has not been investigated.

The drag coefficient C_{dl} or the normalized out-of-phase component of the total instantaneous transverse force given in figures 10, 11, and 12 show that C_{dl} becomes negative for $\bar{V}T/D$ values between approximately 4.5 and 7 (i.e. for normalized frequencies between 0.14 and 0.22). Outside this range the drag is positive, thus in the opposite direction

to the motion of the cylinder. Within the range of $\bar{V}T/D$ values cited above, the drag force is in phase with the direction of motion of the cylinder and helps to magnify the oscillations rather than damp them out. For this reason, the region in which C_{d1} is negative is sometimes referred to as the negative damping region. The fact of the matter is that this is not damping in the proper use of the word but rather an energy transfer from the fluid to the cylinder via the mechanism of synchronization. The values of $\bar{V}T/D$ at which C_{d1} changes its sign depend on A/D as seen in figures 10, 11, and 12 even though the negative C_{d1} region roughly lies within the $\bar{V}T/D$ values of 4.5 and 7. The envelopes of the two zero crossings determine the region of self excited oscillations. A precise determination of such an envelope and its dependence on the Reynolds number will require experiments with additional A/D values and other Reynolds numbers. For purposes of the present investigation, it suffices to note that the maximum absolute value of C_{d1} in the synchronization range decreases rapidly as A/D increases. Field studies have shown that synchronization does not occur for relative amplitudes larger than unity. The trend of the present data is in conformity with such observations.

Finally, an unexpected and previously unknown observation in connection with the variation of C_{d1} will be described. For normalized frequencies $(D/\bar{V}T)$ smaller than about 0.14 the data yield positive drag coefficients. Between 0.14 and 0.22, the synchronization takes place and the drag coefficient

is negative as noted above. Ordinarily one would have expected that the drag coefficient will remain positive and continue to increase with increasing frequencies beyond $D/\bar{V}T = 0.22$ and eventually reach a value which would be identical to that obtained by oscillating the cylinder in a fluid otherwise at rest. However, an interesting phenomenon takes place at frequencies between approximately 0.22 and 0.27, depending on the A/D ratio. For example for A/D=0.75, C_{dl} increases rapidly at $D/\bar{V}T = 0.26$ and then decreases sharply to nearly zero. At first it was suspected that this might be due to an experimental error. However, the repeatability of the experiments and the observation of the same phenomenon at other relative amplitudes and velocities have shown that there is indeed a dramatic change in C_{dl} at $D/\bar{V}T = 0.26$ for A/D = 0.75, at $D/\bar{V}T = 0.24$ for A/D = 0.5 and at $D/\bar{V}T = 0.31$ for A/D = 0.25. It is further noted from the data presented herein that, particularly for A/D = 0.25 and 0.5, C_{dl} becomes once more negative in a narrower range of $D/\bar{V}T$ values ($D/\bar{V}T$ from 0.345 to 0.45 for A/D = 0.25) and shows the existence of a second region of synchronization. The $D/\bar{V}T$ value at which C_{dl} acquires its second minimum value in the case of A/D = 0.25 is almost exactly twice that of the first minimum. The occurrence of this second region of synchronization at higher frequencies depends on the A/D value. The fact that is demonstrated here is that there is not a single region of synchronization and that there is at least one and possibly more regions of frequency in which synchronization can occur.

The narrowness of the regions of frequency in the second region of synchronization makes it rather difficult to observe the phenomenon. In fact one may easily miss such a region by simply not taking smaller increments in frequency. It suffices to say that a cylinder may be excited first at frequencies near the Strouhal frequency and then at the multiples of the Strouhal frequency. However, the largest energy transfer from the fluid to the cylinder occurs in the first synchronization region near the Strouhal frequency.

V. CONCLUSIONS

The experimental investigation of the transverse oscillations of a cylinder in a flow with an ambient mean velocity $\bar{V}$ has yielded the force coefficients $\bar{C}_{di}$, C_{ml} and C_{dl} and has shown that;

a. The mean flow has significant effects on the force transfer coefficients and that the result of experiments with harmonic oscillations in a fluid otherwise at rest are not applicable to the transverse oscillations of a cylinder in a uniform flow;

b. It is possible to excite transverse oscillations for A/D smaller than about unity. In a region of $D/\bar{V}T$ in the vicinity of the Strouhal frequency, the out-of-phase component of the total force becomes negative and some energy is transferred from the fluid to the cylinder. The rate at which energy is transferred decreases with increasing relative amplitudes. Furthermore there is at least one, and possibly more, narrower bands of frequencies at which synchronization occurs.

c. Transverse oscillations give rise to an increased drag force in the direction of the mean flow. This force depends on A/D as well as on $D/\bar{V}T$ and reaches a maximum at about $D/\bar{V}T = 0.18$. This value corresponds to a normalized frequency slightly below the Strouhal frequency and is well within the synchronization region. From a practical point of view this is a matter of concern for sound design of cables

and other structures which may be subjected to transverse oscillations;

d. A meaningful dynamic analysis of the vortex excited transverse oscillations may be carried out only through the use of the force transfer coefficients presented herein. However, it is necessary that additional data be obtained at other amplitudes and Reynolds numbers. Furthermore, additional experiments may also have to consider the roughness of the oscillating structure.

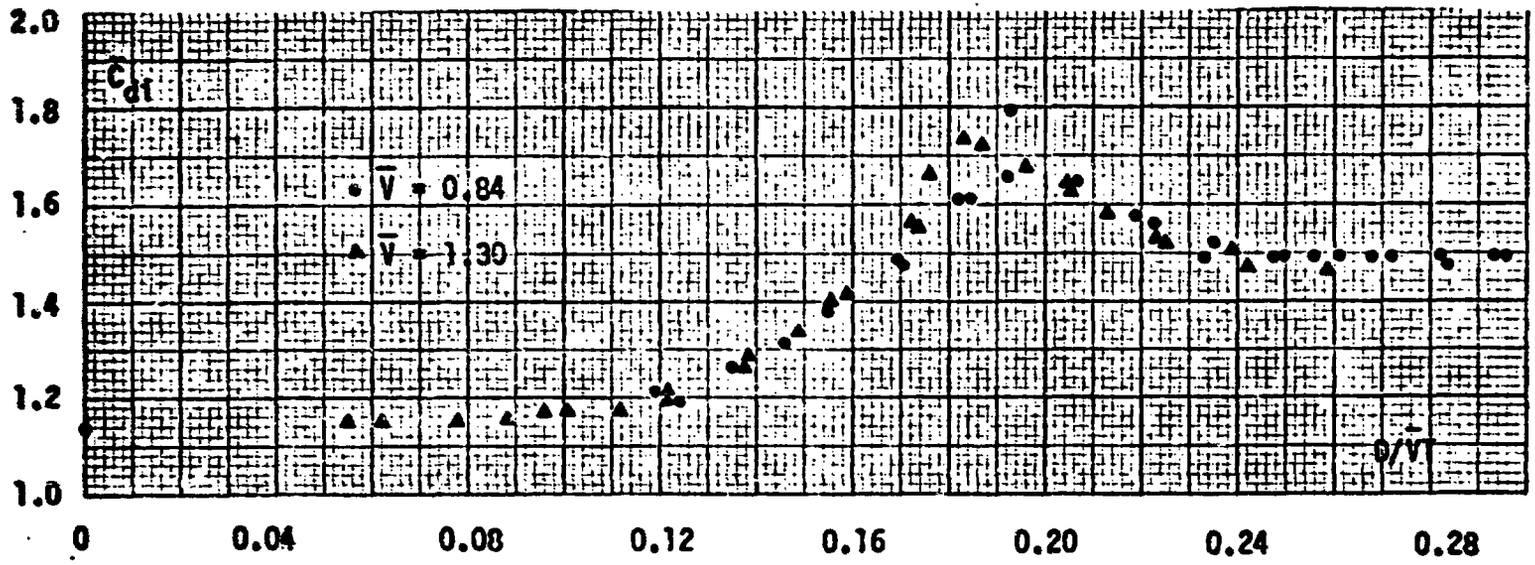

Fig. 5 Mean in-line drag coefficient versus D/$\bar{V}$T for A/D = 0.25

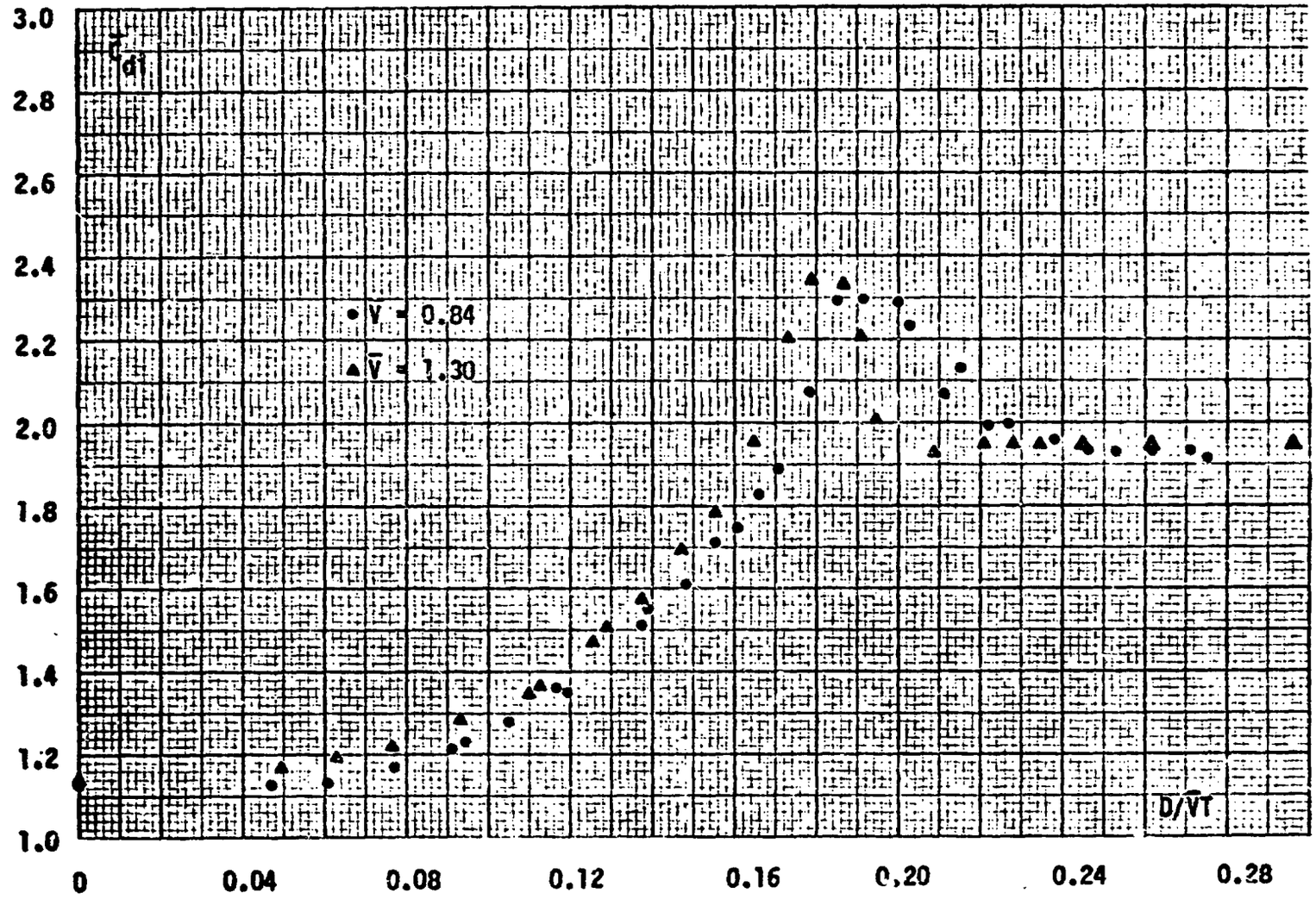

Fig. 6 Mean in-line drag coefficient versus D/$\bar{V}$T for A/D = 0.50

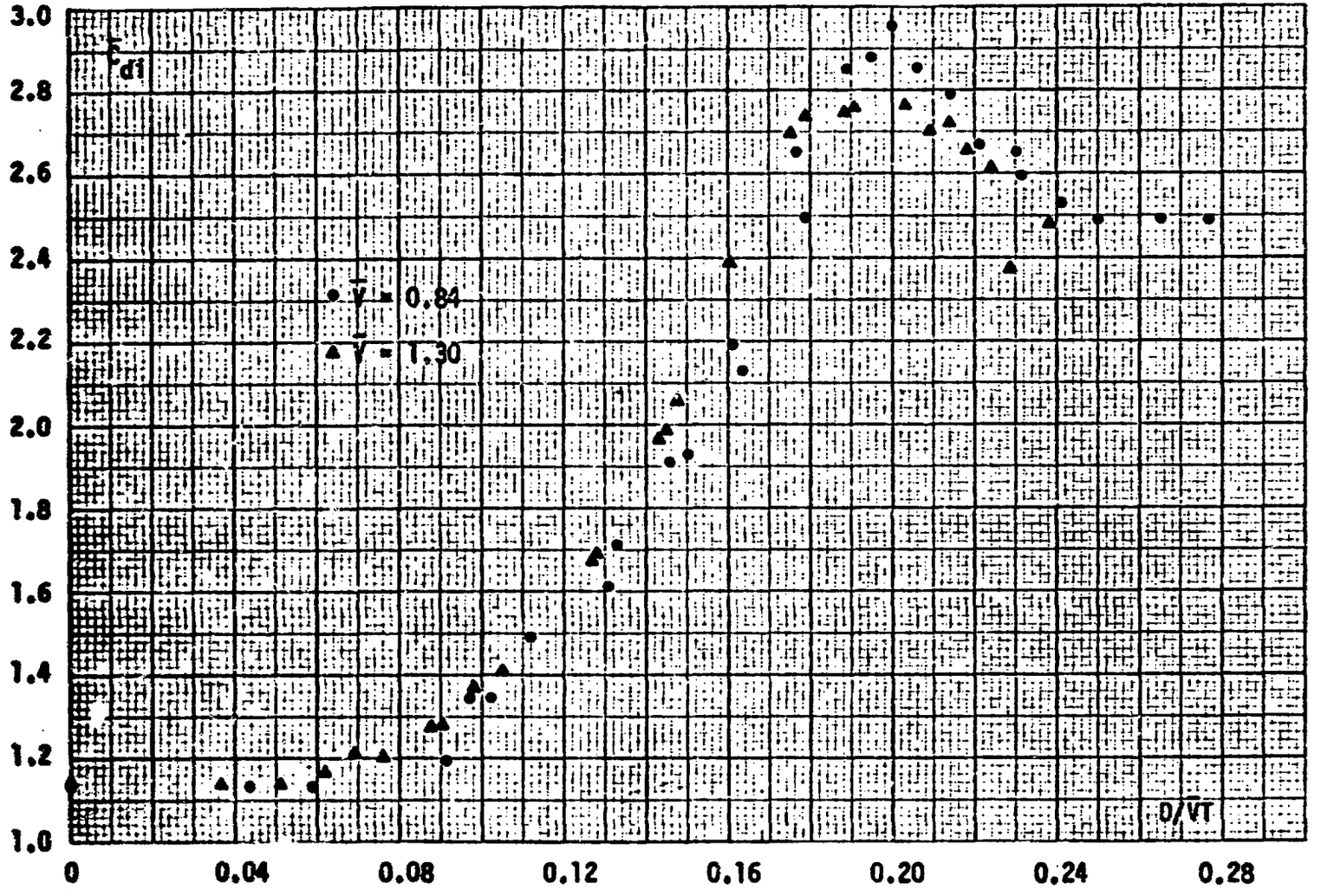

Fig. 7 Mean in-line drag coefficient versus D/$\bar{V}$T for A/D = 0.75

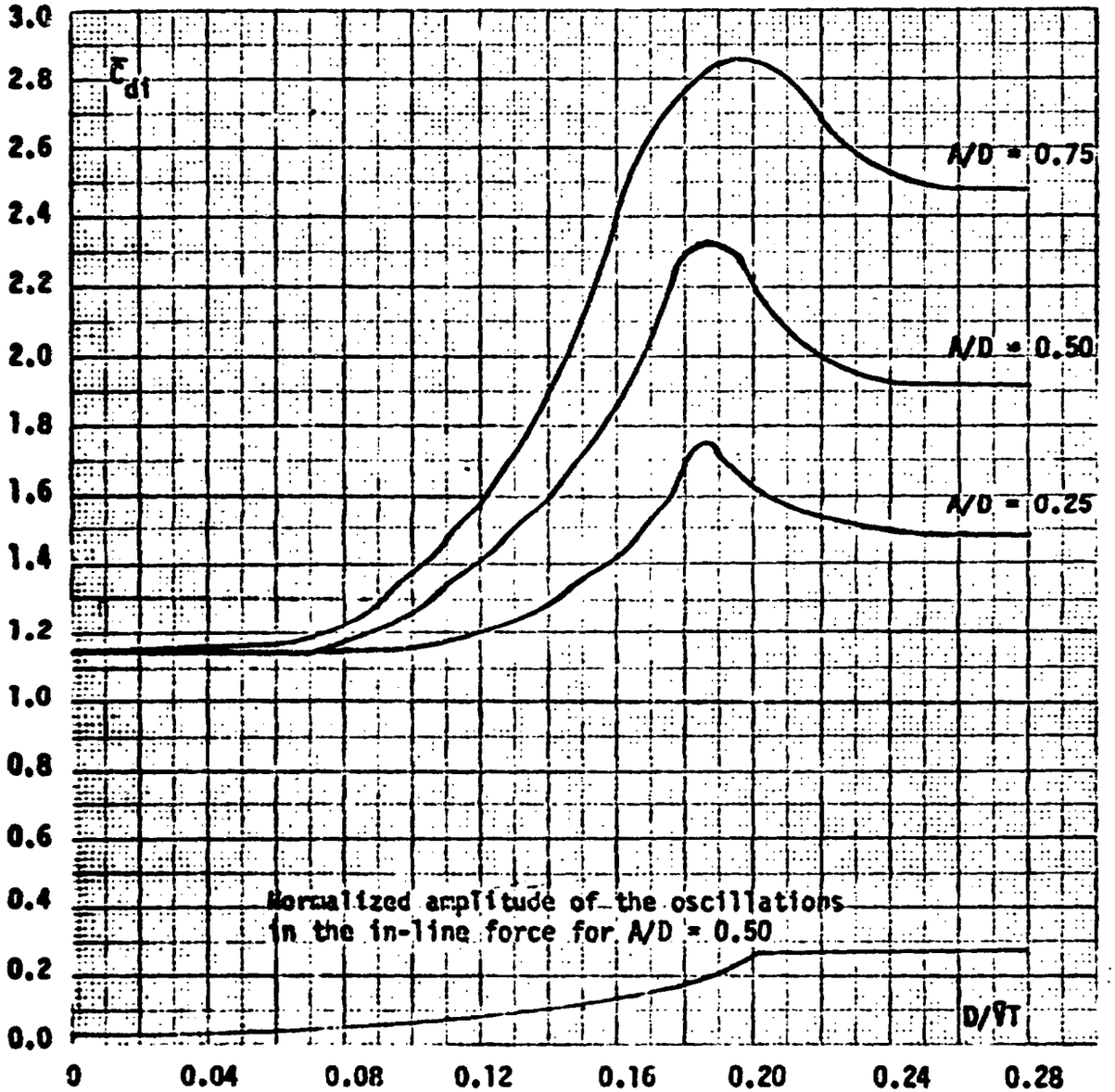

Fig. 8 Comparison curves: Mean in-line drag coefficient versus $D/\overline{V}T$ for A/D = 0.25, 0.50, 0.75

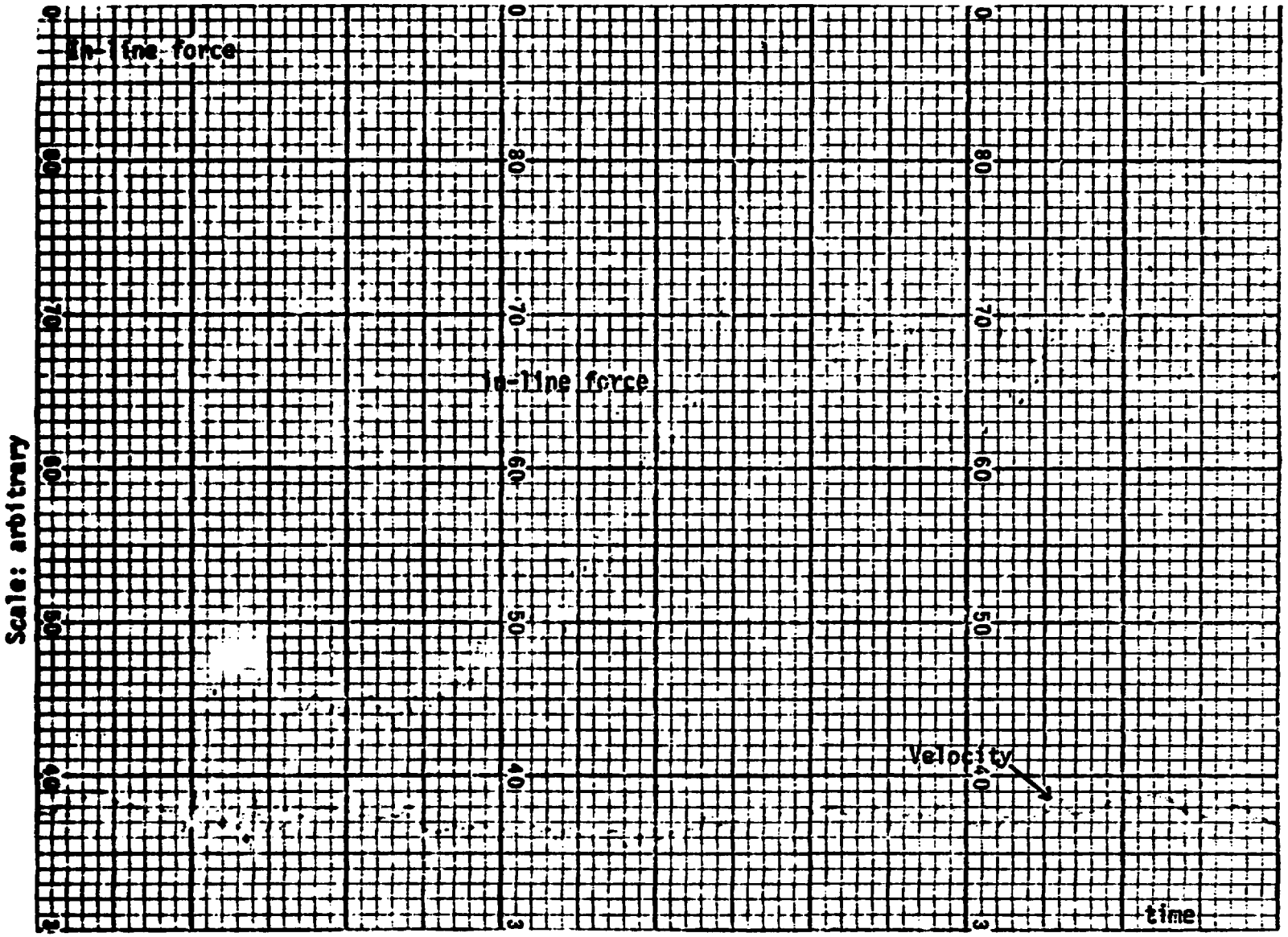

Fig. 9 Phenomenological Demonstration: In-line force versus time while increasing oscillation frequency, (A/D = 0.50, V = 0.84, $D/\bar{V}T$ = 0 to 0.31).

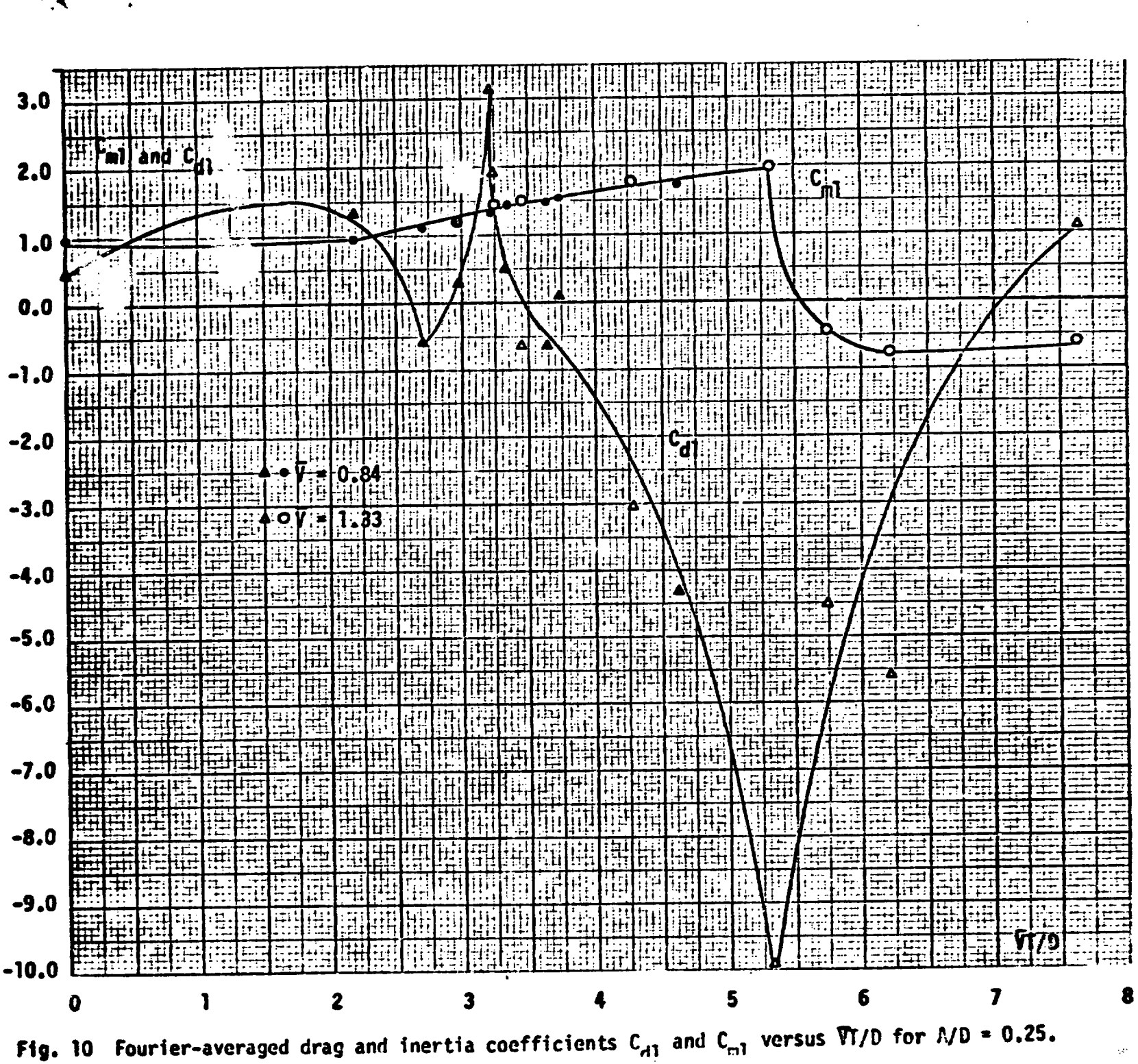

Fig. 10 Fourier-averaged drag and inertia coefficients C_{d1} and C_{m1} versus $\bar{V}T/D$ for $A/D = 0.25$.

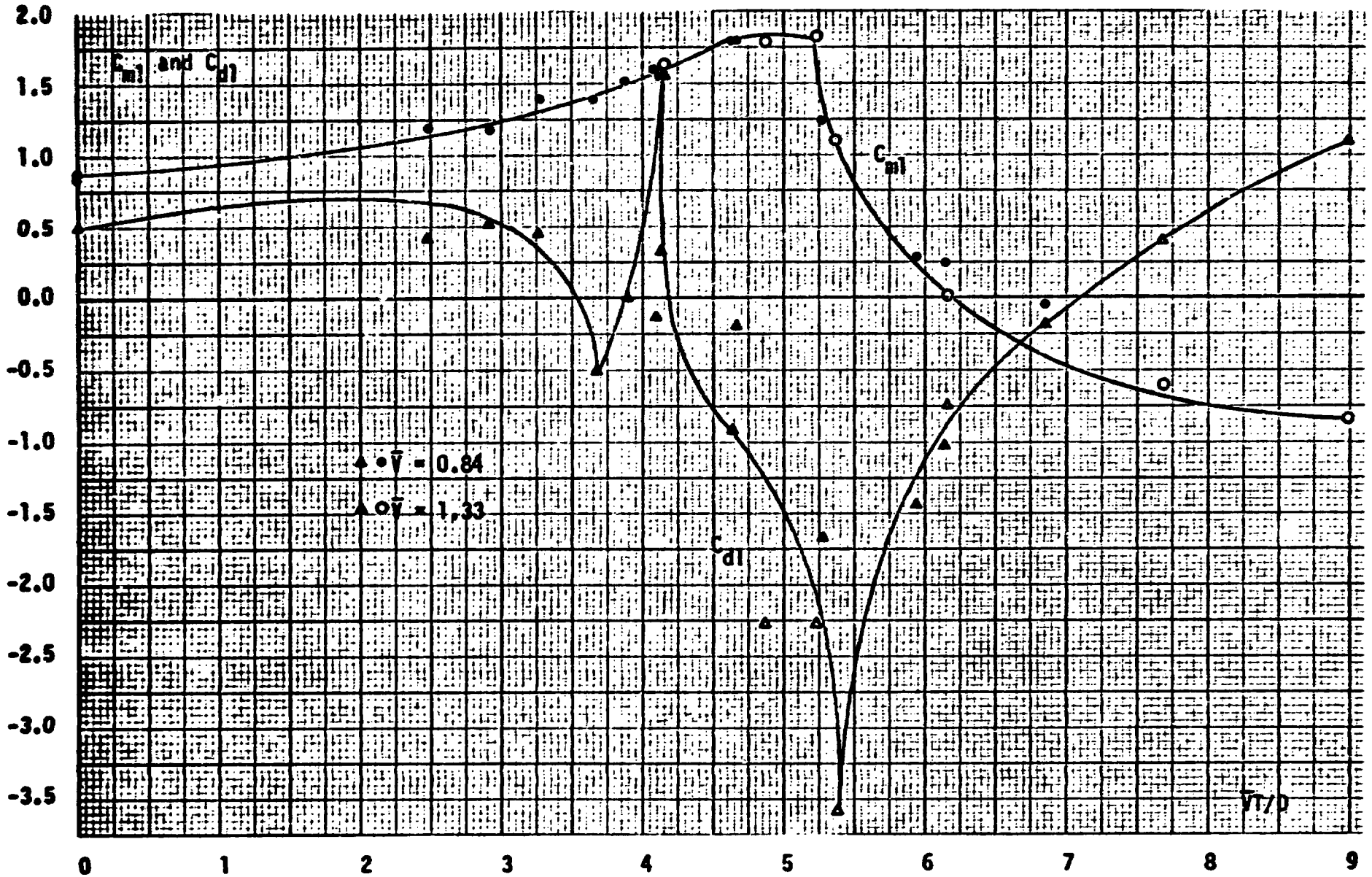

Fig. 11 Fourier-averaged drag and inertia coefficients C_{dl} and C_{ml} versus $\bar{V}T/D$ for A/D = 0.50.

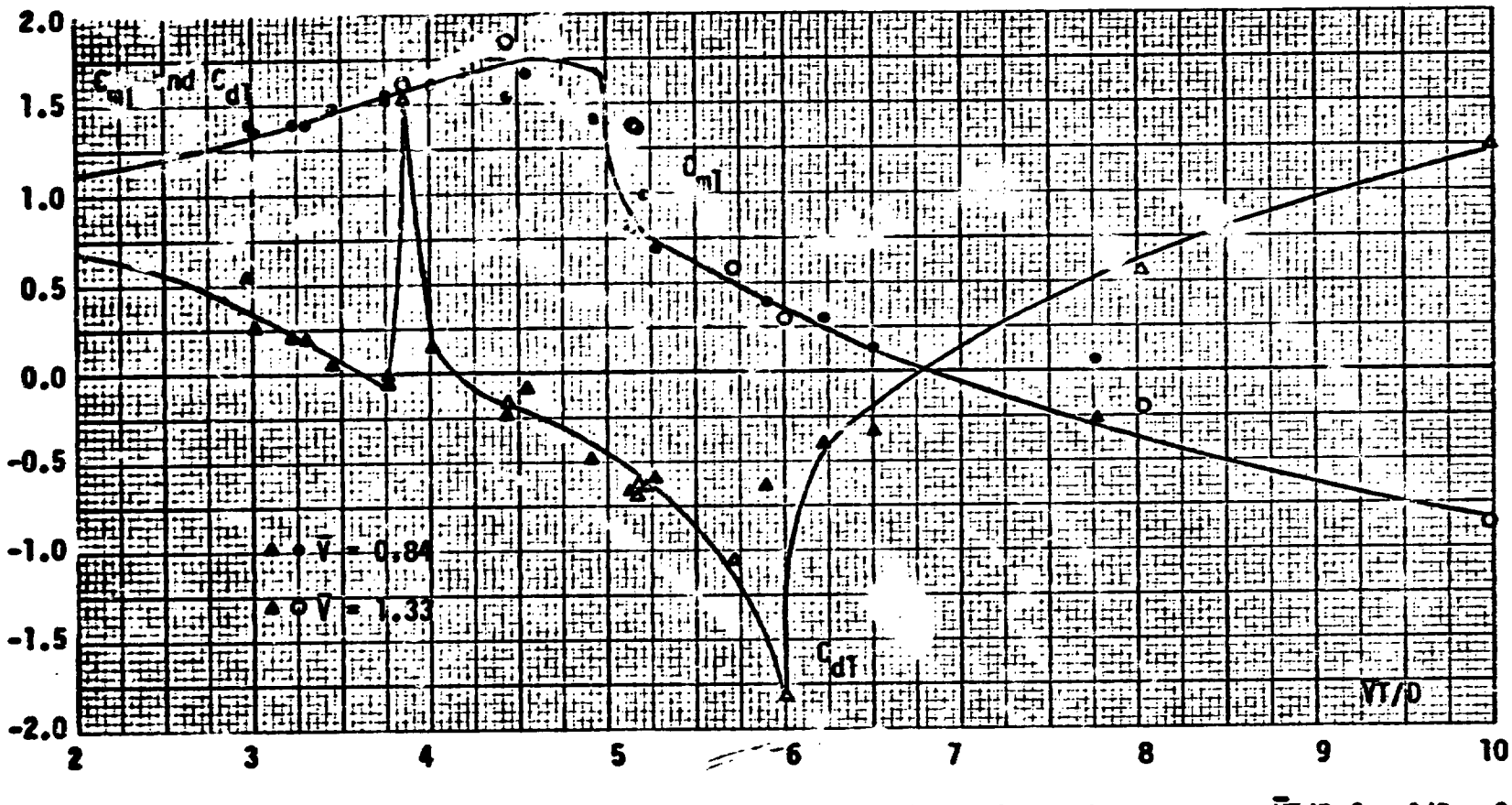

Fig. 12 Fourier-averaged drag and inertia coefficients C_{dl} and C_{ml} versus $\bar{V}T/D$ for $A/D = 0.75$.

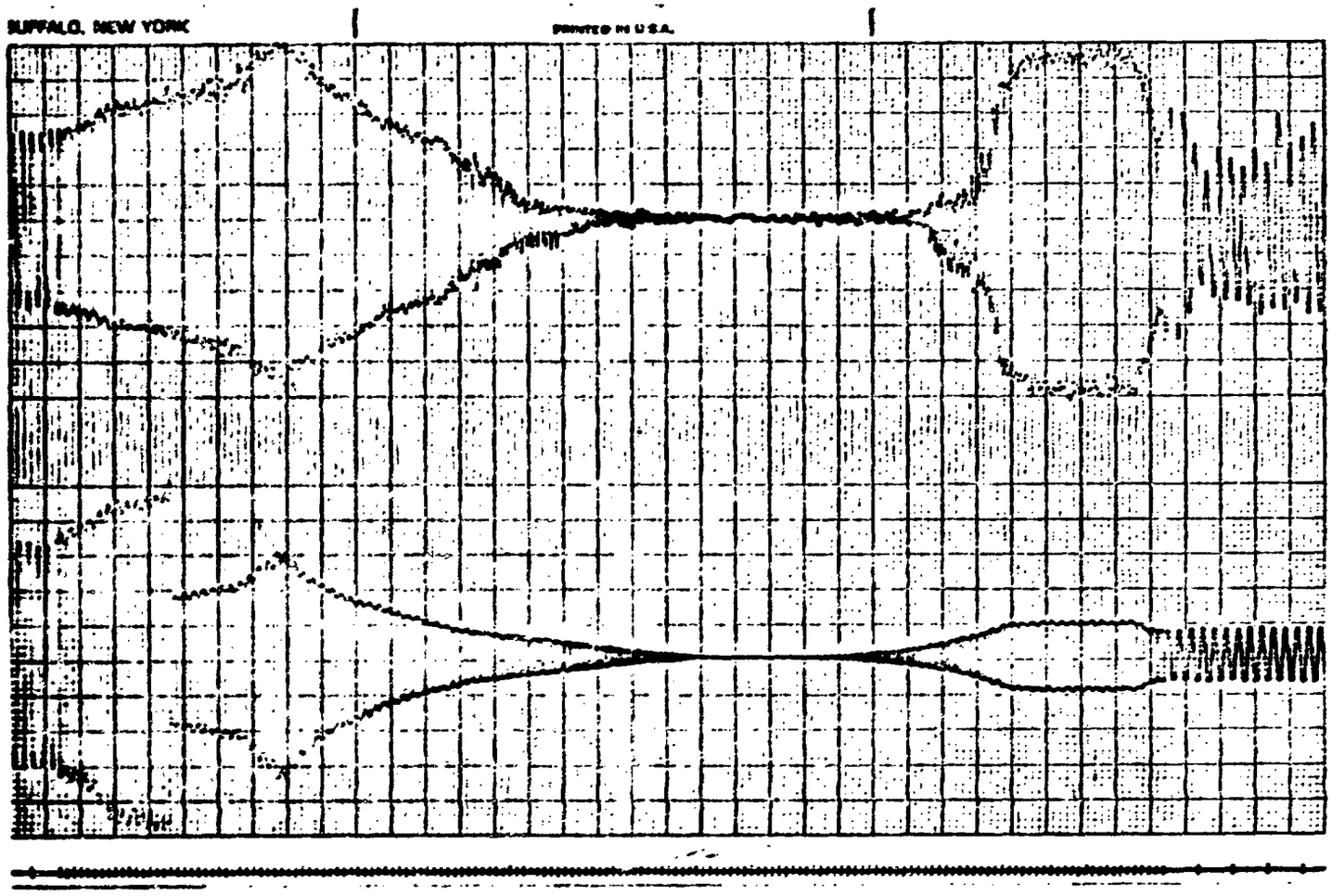

Fig. 13a Phenomenological demonstration: Transverse force versus time while increasing the oscillation frequency

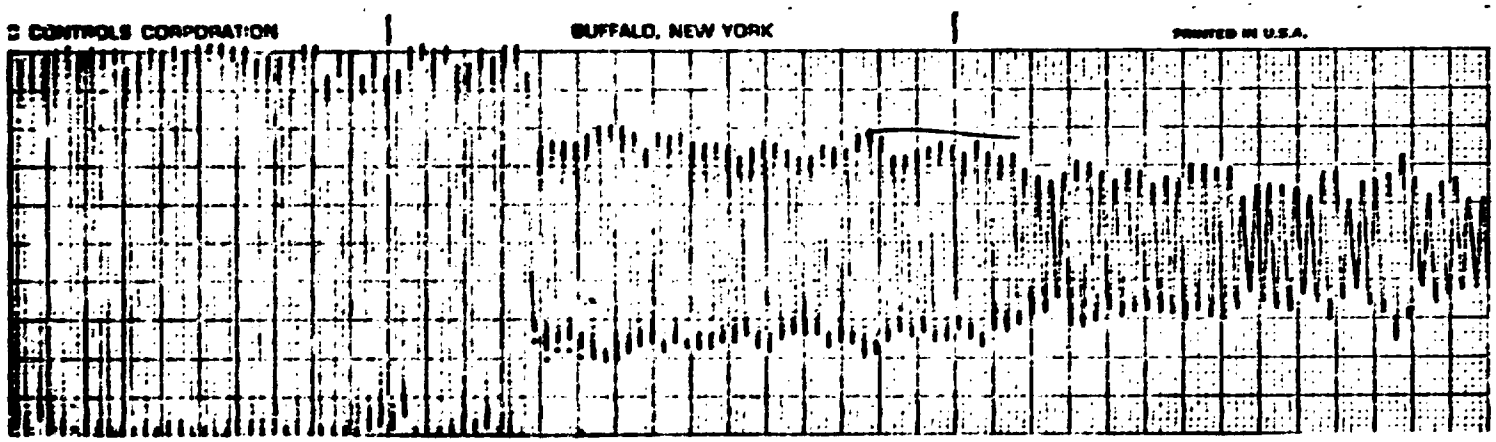

Fig. 13b Phenomenological demonstration: Transverse force versus time while increasing the oscillation frequency

APPENDIX A

COMPUTER PROGRAM

```
CCCCCCCCCCCCCCCCCCCCCCCCCCCCCCCCCCCCCCCCCCCCCCCCCCCCCCCCCC
C                                                       C
C      [illegible] CALCULATIONS FOR CYLINDERS           C
C      TIME=[illegible] TIME (TIME/PERIOD)              C
C      [illegible]=DIMENSIONLESS DISPLACEMENT(UMAX*PER/DIA) C
C      V[illegible] DIMENSIONLESS FREQUENCY PARAMETER   C
C      CL=CYLINDER LENGTH IN FEET                       C
C      DIA=DIAMETER OF CYLINDER IN FEET                 C
C      AMP=AMPLITUDE OF MOTION IN FEET                  C
C      PER=PERIOD IN SECS (CHART PERIOD/CHARTSPEED)     C
C      Z[illegible] COEFFICIENTS                        C
C      F[illegible]= FORCE IN CHART UNITS               C
C      F[illegible]=[illegible] FORCE IN CHART UNITS    C
C      FMAX=MAXIMUM DRY FORCE IN CHART UNITS            C
C      F[illegible]=AVERAGE WET FORCE IN CHART UNITS    C
C      FDMEAN=AVERAGE DRY FORCE IN CHART UNITS          C
C      [illegible] COEFFICIENT                          C
C      CD=DRAG COEFFICIENT                              C
C      N=NUMBER OF DATA SETS                            C
C      CN=CONVERSION FACTOR                             C
C                                                       C
CCCCCCCCCCCCCCCCCCCCCCCCCCCCCCCCCCCCCCCCCCCCCCCCCCCCCCCCCC
      DIMENSION FORCE(300),FWET(300),FMAX(20),SINA(300),COSA(300)
C     READ THE PARAMETERS WHICH CHARACTERIZE THE DATA SET
C
      [illegible]=1
      DO [illegible] I=1,[illegible]
      READ(5,1)(DIA,AMP,PER,NCARD,UMX,CN,FNMAX,NRUN,NDRY
      CYCL=[illegible])
      [illegible]AX=[illegible]CYCLE+1
      READ(5,55)(FMAX(K),K=1,[illegible]AX)
      READ(5,55)(FWET(K),K=1,NCARD)
      READ(5,55)(FORCE(K),K=1,NDRY)
      G=32.174
      [illegible]
      PI=3.1415[illegible]
      [illegible]
      CL= .[illegible]
      VF[illegible]=1.[illegible]
      [illegible]=([illegible])/([illegible]*CYCLE))+0.499
      Y=[illegible]/(2.0*CYCLE)
      [illegible] DATA SETS
C
C
C     COMPUTE FORCE COEFFICIENTS
      Z[illegible]=([illegible]*PER*C[illegible])/(P[illegible]*DIA*DIA*DIA*CL*RHO*AMP)
      Z[illegible]=-([illegible]*C[illegible])/(RHO*DIA*DIA*CL*AMP*AMP)
      [illegible]
      [illegible]/DIA
      [illegible]=(V[illegible]*DIA)/C[illegible]
      WRITE(6,15)DIA,AMP,PER,UMX,CN,NRUN
      WRITE(6,23)
      [illegible]
      FDMEAN=0.0
      DO 15 K=1,NCARD
      [illegible](K)
      FDMEAN=FDMEAN+FORCE(K)
   15 CONTINUE
      [illegible]/NCARD
      FDMEAN=FDMEAN/NCARD
      DO 94 K=1,NDRY
      FORCE(K)=-(FORCE(K)-FDMEAN)
   94 CONTINUE
      DO 97 K=1,NCARD
      FWET(K)=-(FWET(K)-FMEAN)
   97 CONTINUE
      DO [illegible] K=1,[illegible]AX
      FMAX(K)=ABS(FMAX(K)-FDMEAN)
   9[illegible] CONTINUE
      CD[illegible]=0.0
      S[illegible]V/(VPA[illegible]PER)
      V[illegible] = VP[illegible]PER/DIA
      TIME=0.0
```

```
      C(K)=0.0
      S(K)=0.0
      CSA=0.0
      SNA=0.0
      FMMM=0.0
      FMFT=0.0
      FCOSA=0.0
      DELTAT=(VCLE/SCNFO
C
C     COMPUTE SINE FUNCTION
      FLI=IDV-1
      DO 22 K=1,FLI
      F=(FREQ(K)+FREQ(K+1))/2.0
      DO 33 L=1,NMAX
      IF(F.GT.(Y*(L-1)).AND.F.LE.(Y*L))FMMM=FMAX(L)
   33 CONTINUE
      S(K)=F/FMMM
      TIME=TIME+DELTAT/2.0
      J=(K/2)-1
C     EVALUATE FOURIER COEFFICIENTS
C
      DO 222 K=1,J
      DO 44 L=1,NMAX
      IF((F.GT.(Y*(L-1)).AND.F.LE.(Y*L))FMFT=FMAX(L)
   44 CONTINUE
      F=(FREQ(K)+FREQ(K+1))/2.0
      CSA=CSA+F
      SNA=SNA+SINA(K)*S(K)
      C(K)=(1.0/F)
      CSA=CSA+(COSA(K))*COSA(K)*COSA(K)
      FCOSA=COSA(K)
      FSIN=SINA(K)
      FDCOS=FDCOS+C(K)
      FDSIN=FDSIN+S(K)
      FCOSA=CSA
      WRITE(6,33)TIME,COSA(K),SINA(K),F,FDCOS,FDSIN,FMMM,FMFT,FCOSA,FSIN
C
      TIME=TIME+DELTAT
  222 CONTINUE
```

```
      K=NCARD
      F=(FOC(1)+FOC(NCARD))/2.0
      CO=A(K)=SINA(K+1)
      SINA(K)=SINA(K)+SINA(K)*SINA(K)
      COSA(K)=COSA(K)+COSA(K)*COSA(K)*COSA(K)
      FDSIN=FDSIN+SINA(K)
      FDCOS=FDCOS+COSA(K)
      CD=FDCOS+CD
      CM=CM+F
      FNET=((FNET(1)+FNET(NCARD))/2.0)-F
      FSIN=FSIN+FNET*SINA(K)
      FCOSA=FCOSA+FNET*COSA(K)
      CMW=CMW+FSIN
      CDW=CDW+FCOSA
      FMEAN=F
      CM=CM+FMEAN
      CA=CN*COS(A)
      CMW=CMW*(CAP/NCARD)
      CD=CD*((DIA**2.0)/2.0)*DELTA*CL
      CA=CA+CD/2
      WRITE(6,31) DIF,COSA(K),SINA(K),F,FDCOS,FDSIN,FMEAN,FNET,FCOSA,FSIN
   6
      STPH=STPH*(3.0*PI/NCARD)
      CDBAR=CDBAR*(3.0*PI/NCARD)
      ZI=ZI/CYCLE
      Z2=Z2/CYCLE
      VPTOD=2.0*PI*VPTIP
      CD=CD*DELTAT
      CMW=CMW*DELTAT

      CDW=CDW*DELTAT
      FMS=CA*15
      CFMAX=FMAX-CM/C2
      CA=CA/CYCLE
      CD=CD/CYCLE
      CMW=CMW/CYCLE
      CDW=CDW/CYCLE
      WRITE(6,11)
      WRITE(6,33)
      WRITE(6,43)CM,CD,BETA,REYNO,CMW,CDW
      WRITE(6,42)
      WRITE(6,43)STPH,CDBAR,VPTOD,FMEAN,FDMEAN,RMS,CFMAX
      WRITE(6,45)
      WRITE(6,75)STNS,CONS,Z1,Z2
      WRITE(6,11)
  100 CONTINUE
   10 FORMAT(3F4.4,I3,I6.4,F10.6,F8.4,I7,I5)
   11 FORMAT('0',3X,75('*'))
   15 FORMAT('1',2X,'DIA=',F8.4,2X,'AMP=',F8.4,2X,'PER=',
     1F6.4,2X,'VEL=',F8.4,2X,'CM=',F8.4,2X,'RUN=',I6)
    2 FORMAT('0',2X,'TIME/PER',5X,'COSA',6X,'SINA',9X,'F',5X,'FDCOS',5X,
     1'FDSIN',5X,'FMEAN',6X,'FNET',6X,'FNCOS',5X,'FNSIN')
   30 FORMAT('0',12F10.4)
   35 FORMAT('0',7X,'CM=',9X,'CD=',8X,'BETA=',6X,'REYND=',8X,
     1'CMW=',7X,'CDW=')
   40 FORMAT('0',6F12.4)
   42 FORMAT('0',7X,'STPH=',5X,'CDBAR=',7X,'VPTOD=',7X,'FMEAN=',7X,
     1'FDMEAN=',5X,'RMS=',7X,'CFMAX=')
   43 FORMAT('0',7F12.4)
   55 FORMAT('0',10.4)
   65 FORMAT('0',7X,'STNS=',5X,'CONS=',8X,'Z1=',9X,'Z2=')
   75 FORMAT('0',4E12.4)
      STOP
      END
```

LIST OF REFERENCES

1. Parkinson, G.V., "Mathematical Models of Flow-induced Vibrations on Bluff Bodies," Flow-Induced Structural Vibrations (ed. Eduard Naudascher), Springer-Verlag, Berlin, 1974, pp. 81-127.

2. Currie, I.G., Hartlen, R.T., and Martin, W.W., "The Response of Circular Cylinders to Vortex Shedding," Flow-Induced Structural Vibrations (ed. Eduard Naudascher), Springer, Verlag, Berlin, 1974, pp. 128-157.

3. Hartlen, R.T. and Currie, I.G., "Lift-Oscillator Model of Vortex-Induced Vibration," Proc. ASCE, EMS, Oct. 1970, pp. 577-591.

4. Morison, J.R., et al., "The Force Exerted by Surface Waves on Piles," Petroleum Trans., Vol 189, 1950, pp. 149-157.

5. Wiegel, R.L., Oceanographical Engineering, Prentice-Hall, Inc., Englewood Cliffs, N.J., 1964, pp. 256-264.

6. Keulegan, G.H. and Carpenter, L.H., "Forces on Cylinders and Plates in an Oscillating Fluid," Journal of Research, NBS, Vol. 60, 1958, pp. 423-440.

7. Sarpkaya, T., "Forces on Cylinders and Spheres in a Sinusoidally Oscillating Fluid," Jour. of Appl. Mechs. Trans. ASME, Vol. 42, No. 1, 1975, pp. 32-37.

INITIAL DISTRIBUTION LIST

		No. Copies
1.	Defense Documentation Center Cameron Station Alexandria, Virginia 22314	2
2.	Library, Code 0212 Naval Postgraduate School Monterey, California 93940	2
3.	Professor T. Sarpkaya, Code 59 Department of Mechanical Engineering Naval Postgraduate School Monterey, California 93940	2
4.	Lieutenant Commander David W. Meyers 296 Payne Avenue North Tonawanda, New York 14120	2
5.	Department of Mechanical Engineering Naval Postgraduate School Monterey, California 93940	2